International Journal of Applied Pharmaceutics

ISSN- 0975-7058 Vol 15, Issue 4, 2023

Original Article

APPLICATION OF PLACKETT-BURMAN AND BOX-BEHNKEN DESIGNS FOR SCREENING AND OPTIMIZATION OF ROTIGOTINE HCL AND RASAGILINE MESYLATE TRANSFERSOMES: A STATISTICAL APPROACH

SHIVANI PATEL[1*], LALIT LATA JHA[2]

[1*]Department of Pharmaceutics, Faculty of Pharmacy, Parul University, P. O Limda, Tal. Waghodia, Vadodara-391760, Gujarat, India.
[2]School of Pharmacy, Parul University, P. O Limda, Tal. Waghodia, Vadodara-391760, Gujarat, India
*Corresponding author: Shivani Patel; *Email: rapatelshivani@gamil.com

Received: 24 Feb 2023, Revised and Accepted: 20 Apr 2023

ABSTRACT

Objective: The objective of this study was to optimize the transferosomal formulation containing Rotigotine HCL(RTG) and Rasagiline mesylate (RSM) and to identify the significant factors affecting particle size and entrapment efficiency.

Methods: The optimized batch was characterized using various techniques, such as TEM to confirm the shape of vesicles and FTIR analysis to check the compatibility of the formulation. The vesicle size of the transferosomes was determined using a zeta sizer. The entrapment efficiency of both drugs was also determined. *In vitro* drug permeation investigation was carried out from the optimized batch to determine the cumulative permeation rate after 24 h. The study also evaluated the deformability index of the transferosomes.

Results: The results showed that transferosomes were spherical particles with a uniform distribution and suitable for drug delivery. The vesicle size of the transferosomes was in the range of 54.05-167.98 nm and 66.02-184.04 nm for RTG and RSM transferosomes, respectively. The polydispersity index for RTG transferosomes was observed in the range of 0.242-0.508, the entrapment efficiency of RTG was 45.66-88.96% and RSM was found to be 57.6-92.57%. The *in vitro* drug permeation investigation from the optimized batch showed a cumulative permeation rate of 92.268% of RTG and 87.72% of RSM after 24 h.

Conclusion: The study findings suggest that transferosomes can be a promising drug delivery system for rotigotine HCL and rasagiline mesylate. The optimized batch showed high entrapment efficiency, good permeation rate, and optimal deformability, making it a suitable option for drug delivery.

Keywords: Rotigotine HCL, Rasagiline mesylate, Plackett-burman design, Box-behnken design, Transferosomes, Entrapment efficiency, Zeta potential

DOI: https://dx.doi.org/10.22159/ijap.2023v15i4.47674. Journal homepage: https://innovareacademics.in/journals/index.php/ijap

INTRODUCTION

Rasagiline mesylate and rotigotine HCl are commonly used as first-line treatments for Parkinson's disease, but they face challenges in their effective delivery. RSM, despite being highly water-soluble, has difficulty penetrating through the skin. On the other hand, RTG formulated as a transdermal patch shows poor bioavailability and undergoes first-pass metabolism. To overcome these challenges, vesicular carrier systems such as transferosomes can be used [1-3]. Transferosomes are specialized vesicles consisting of an aqueous core surrounded by a lipid bilayer with an edge activator [4]. These vesicles are ultra-deformable and elastic, allowing them to easily penetrate the skin through minuscule holes or constrictions. The modified liposomal vesicular system used for transfersomes consists of dipalmitoyl phosphatidyl glycerol (DPPG) phospholipids and a single-chain surfactant as an edge activator [5]. The edge activator destabilizes the membrane, increasing the vesicle's deformability and flexibility. When mixed in the appropriate proportion with the lipid component, the resulting mixture produces highly deformable and ultra-flexible transferosomes. This innovative vesicular carrier system can be utilized to facilitate the effective delivery of RSM and RTG and improve their therapeutic efficacy [6-9]. Transfersomes can pass through intact skin without occlusion, and this is achieved by creating a trans-epidermal osmotic gradient across the skin. Hydrotaxis (xerophily) is the permeation mechanism of transfersomes, where they seek moisture in deeper skin layers rather than a dry outer background. When applied to the skin in a non-occlusive condition, the transferosomal formulation undergoes moisture evaporation, leading to the creation of a transdermal water activity differential [9-11].

The identified significant factors from the Plackett burman screening design were used to optimize the formulation with the application of Box Behnken Design. At two levels,+1 and-1, 8 quantitative variables are chosen for the screening. Here, variables X1 to X8 are real, while variables X10 to X12 are dummy or false, do not correspond to any real factors, and are so excluded. The experimental domain thus displays 12 variables across 12 runs. Quantities of lipid, edge activator, hydration media, alcohol, hydration time, temperature, sonication time, and rotation speed are among the variables that need to be examined [12-16].

The Box-Behnken design is a three-level factorial design that involves three factors with three levels each. The design involves selecting a set of experimental conditions based on a statistical approach [17]. In the present study, the vesicle size and entrapment efficiency (EE %) were considered the dependent variables (Y1 and Y2). To investigate the effects of various formulation factors on these variables, we used design-expert version 12.0 software. To obtain an optimized formula that meets our desired outcomes, we generated fifteen runs based on the experimental design. The data collected from the experiments were analyzed using the analysis of variance (ANOVA) test to assess the statistical significance of the model and the results obtained. An interactive and polynomial statistical model was used to analyze the formulation replies, and it is represented by the following equation:

$$Y = b_o+b_1X_1+b_2X_2+b_3X_3+b_{12}X_1X_2+b_{13}X_1X_3+b_{23}X_2X_3+b_{11}X_1^2+b_{22}X_2^2+b_{33}X_3^2$$

Where Y stands for the dependent response and b0 represents the intercept; b1, b2, b3, b12, b13, b23, b11, b22, and b33 stand for the regression coefficients. In addition to X1, X2, and X3, X1X2, X1X3, and X2X3 denote the interactions between the primary elements, whereas X12, X22, and X32 denote the polynomial terms. The independent factors importance on the dependent responses was indicated by the p-values associated with the regression coefficients [18-20].

MATERIALS AND METHODS

Materials

Rotigotine HCl was gifted by Neuland Laboratory Mumbai, Rasagiline mesylate was procured from Benzchem Enterprise Vadodara, Phospholipon 90 G was gifted by lipoid Germany, Sodium Deoxycholate, dihydrogen potassium phosphate, dihydrogen sodium phosphate and sodium chloride were procured Chemdyes Corporation, Rajkot.

Method for preparation of RSM-transferosomes

The transferosomes were produced using the film hydration method. Firstly, a specified quantity of phospholipon 90 G and sodium deoxycholate were dissolved in 10 ml chloroform and placed in a round bottom flask. rotigotine HCl was then added to the mixture. A rotary evaporator was used to create a thin, uniform film. Rasagiline mesylate was dissolved in a 7.4 pH phosphate buffer solution, which was then used to hydrate the lipid film, forming the transferosomes. The vesicles were allowed to hydrate at room temperature for approximately two hours. Subsequently, the hydrated transferosomal solution was sonicated to further reduce the size of the vesicles [21].

Method for preparation of RTG-transferosomes

To prepare the transferosomes using the film hydration method, Phospholipon 90 G and sodium deoxycholate were dissolved in 10 ml chloroform and added to a round bottom flask. Then, rotigotine HCl was added to the mixture. The flask was connected to a rotary evaporator with a round bottom to create a thin, uniform film. Next, a 7.4 pH phosphate buffer solution was added to the film to create a hydrated layer. The vesicles were allowed to hydrate for approximately 2 h at room temperature. Finally, to further decrease the size of the transferosomes, the hydrated solution was sonicated [21].

Characterization

Morphological characterization

The preliminary morphological characterization of the optimized transferosomes was conducted using an inverted microscope at 40X resolution to confirm their shape. The vesicular structure of the optimized transferosomes was further confirmed using TEM with different resolutions. To conduct a thorough morphological analysis of the improved RSM and RTG-loaded transferosomal formulation, a negative staining approach was employed. One drop of the aqueous dispersion was placed on a carbon-coated copper grid, and any excess dispersion was removed with filter paper after one minute. The sample was then exposed to a 1% phosphotungstic acid solution and allowed to dry at room temperature before being examined at 100 kV [22].

Polydispersity index (PDI), Zeta potential, and Vesicle size (VS) Evaluation (ZP)

The polydispersity index (PDI), zeta potential (ZP), and vesicle size (VS) were evaluated using a zeta sizer (Malvern zeta sizer, Malvern instruments Ltd.) to determine the stability and quality of the formulated transferosomes. These parameters are important characteristics for selecting the optimum transfersomal formulation. The measurements were taken using double distilled water as a diluent at a temperature of 25 °C [23, 24].

FTIR study of transferosomes

To ensure that the drug and excipients in the transferosomal formulation are compatible, FTIR characterization is conducted. The FTIR spectrum of the transferosomal dispersion is scanned and compared to the typical spectra of the drugs to identify any significant differences or changes. This analysis confirms the compatibility of the drug and excipients in the transferosomal formulation, which is crucial for ensuring the effectiveness and safety of the drug delivery system [24].

Entrapment efficiency

To determine the entrapment efficiency (EE), a transferosomal solution equivalent to 1 mg of active pharmaceutical ingredient (API) was placed in a centrifuge tube and centrifuged using a cooling centrifuge at 1500 rpm for 15 min at 4 °C. The supernatant was collected and filtered using Millipore filters with a pore size of 0.45 µm. The concentration of RSM was determined at 239 nm, where RTG shows a zero-crossing point, and the concentration of RTG was determined at 273 nm, where RSM shows a zero-crossing point, using the first-order derivative method. The following equation was used to determine the %EE:

$$\text{Entrapment efficiency} = \frac{\text{amount entrapped}}{\text{total amount added}} * 100$$

Where the amount entrapped is the difference between the total amount added and the amount of API found in the supernatant after centrifugation and filtration. This method helps to determine the percentage of drug that is encapsulated in the transferosomes [25].

In vitro drug permeation studies

A dialysis tube was filled with one ml of transferosomal formulation after being completely sealed on both sides. The tube used for dispersion was submerged in 200 ml of phosphate buffer 7.4 pH at 37 °C were used. The entire assembly was fixed to a magnetic stirrer, and a magnetic bead supplied constant agitation. 5 ml of aliquots were taken from the dissolution liquid at various time intervals and were then the absorbance for RSM at 239 nm where RTG shows zero crossing point and RTG at 273 nm where RSM shows zero crossing point in first-order derivative method to find concentration. After each sampling, an equivalent quantity of PB 7.4 was added to the medium to mimic sink conditions. The total amount of drugs released throughout the course of predetermined time periods was calculated [26].

% Deformability index

The capacity of transferosomes to pass through the skin's tiny channels while maintaining their size and shape depends in large part on a property known as deformability. The deformability of the formulation was measured using an extrusion measuring technique a side hole on the side of a conical flask was fixed with a vacuum pump, but the mouth of the flask was fixed with a rubber bung connected to a stainless-steel flask holder. The formulation was let to flow through a membrane filter with a 0.20 m pore size that was retained on a mesh plate. Readings were recorded in triplicate [27, 28]. The % deformability was calculated by the following equation:

$$D = J\left(\frac{rv}{rp}\right)^2$$

Where D = Deformability index, J = Amount of extruded transferosomal suspension, rv = vesicular size of transferosomes after extrusion, rp = pore size of membrane

Stability studies

The study aimed to assess the effect of storage at 4±2 °C for three months on the optimized RTG and RSM-loaded transferosomal formulation along with the respective optimized transferosomal formulation. The evaluation of various parameters, including VS (vesicle size), and %EE (percent encapsulation efficiency), was performed for the optimized transferosomal formulation at the end of the study period. The evaluation of these parameters after storage can provide valuable information on the stability and integrity of the transferosomal formulation over time. Any changes in these parameters can indicate potential issues such as destabilization of the vesicle structure, or drug leakage from the vesicles [20].

RESULTS AND DISCUSSION

Results of screening study

The study used trial batches to document the outcomes and determine the effects, b0, and sb2 values using a provided formula. Based on the comparison of the effects with the values of b1 to b11, it was found that three factors-the amount of lipid, the amount of edge activator, and the sonication period-were significant for both particle size and entrapment efficiency. The value of sb2 for entrapment efficiency was 3.44366, and three factors showed b values higher than this value. Similarly, the value of sb2 for particle size was 5.747432, and three factors exhibited b values higher than

this value (table 1). The results of the study were presented using a Pareto chart in fig. 1 and 2, which is a graphical representation of the relative importance of different factors in contributing to the observed variation in the response variables. It is used to identify the significant factors and prioritize them for further investigation and optimization.

Table 1: Results of packet-barman (Hadamard) design

Parameters	Parameters	Vesicle size	%EE
Average	B0	86.834	51.083
Amount of lipids	B1	21.614	-9.583
Amount of E. E	B2	6.463	-5.083
Amount of hydration media	B3	3.078	-2.417
Amount of alcohol	B4	-0.306	0.25
Hydration time	B5	1.326	-0.083
Temperature	B6	4.206	-1.417
Sonication time	B7	-5.961	3.917
Rotation speed	B8	-4.571	3.25
Sb^2	Sb^2	5.747	3.444

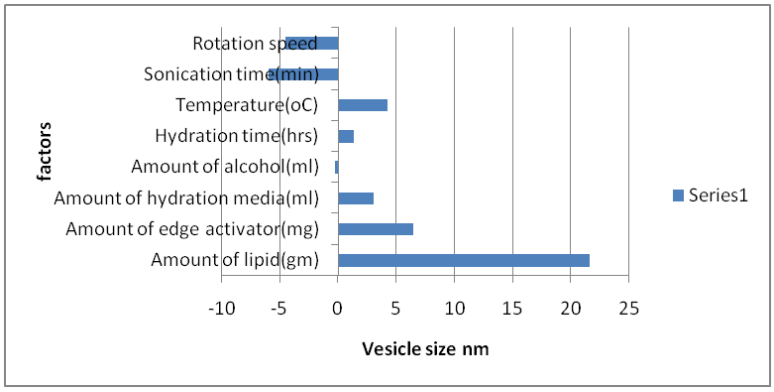

Fig. 1: Pareto chart of factors affecting vesicle size

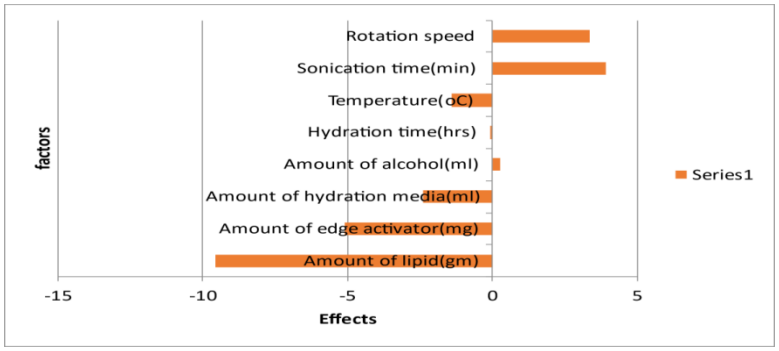

Fig. 2: Pareto chart of factors affecting %EE

Results of optimization of formulation

Morphological characterization

TEM analysis was performed on the sample using a transmission electron microscope operated at 200 and 500 nm resolutions. The images obtained at 200 nm resolution revealed that the particles were spherical in shape with an average diameter of 160 nm. At 500 nm resolution, the particles appeared larger, with an average diameter of 140 nm. The images obtained at both resolutions showed a uniform distribution of particles throughout the sample.

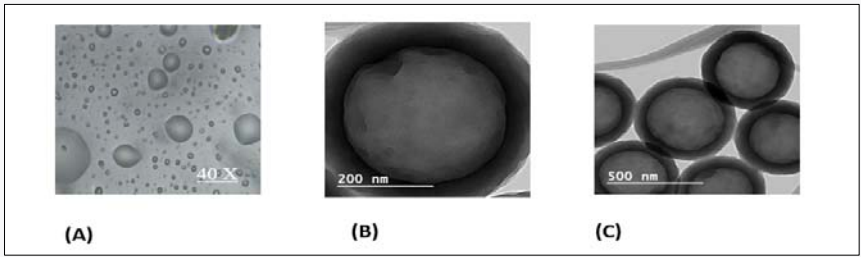

Fig. 3: A. Image of optimized formulation under inverted microscope at 40X B and C Image of optimized formulation under TEM at 200 and 500 nm

FTIR studies

The FTIR spectra of RTG and RSM transferosomes were obtained to analyze the functional groups present in the formulations. The FTIR spectra of RTG and RSM transferosomes are shown in fig. and are interpreted with FTIR spectra of standard drugs. Overall, the FTIR analysis confirmed the presence of the expected functional groups in both RTG and RSM transferosomes.

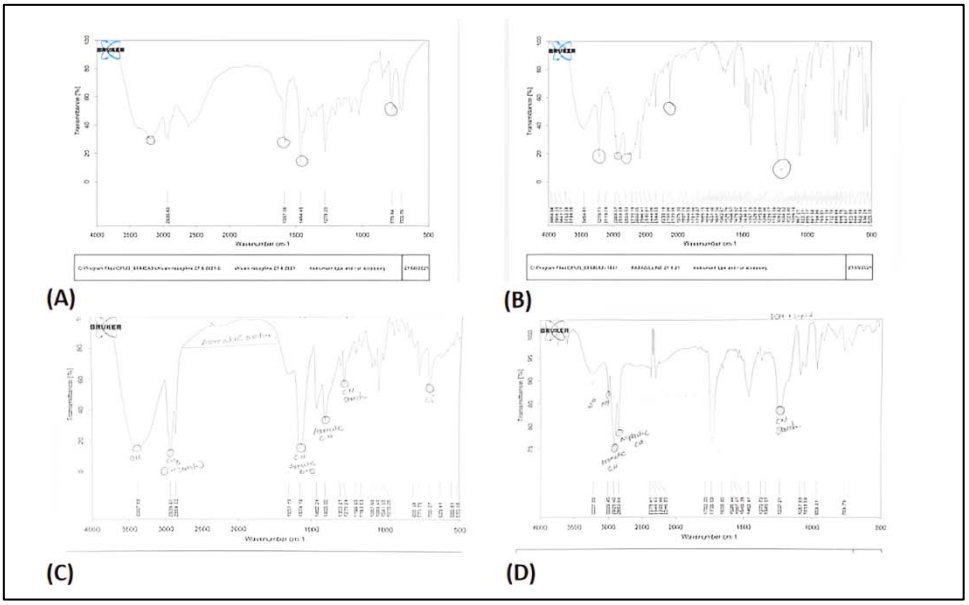

Fig. 4: A. FTIR spectra of RTG B. FTIR spectra of RTG transfersomes C. FTIR spectra of RSM D. FTIR spectra of RSM transferosomes

Particle size

The results of the particle size and distribution of transferosomes containing RTG and RSM can be compared with other studies that have investigated similar transferosome formulations. For instance, a study reported in [29] that transferosomes containing curcumin had a particle size range of 50-150 nm and a PDI range of 0.2-0.4, which is comparable to observed findings. Additionally, a study by [30] reported that transferosomes containing ibuprofen had a particle size range of 100-200 nm and a PDI range of 0.2-0.5, which is slightly larger than the results. The desired particle size for better transdermal diffusion is below 200 nm. The vesicle size of RTG transferosomes was observed to be in the range of 54.05-167.98 nm and RSM transferosomes was observed in the range of 66.02-184.04 nm, which indicates that some formulations meet the desired size range. The PDI for RTG transferosomes was observed in the range of 0.242-0.508 and PDI for RSM transferosomes was observed in the range of 0.224-0.494, which suggests that the particle size distribution was moderately broad. As the amount of lipid increased from 0.5 to 1.5 g, the vesicle size significantly increased from 54.05-167.98 nm and 66.02-184.04 nm for RTG and RSM transferosomes, the observation of work states that concentration of surfactant has a negative correlation effect on vesicle size can be supported by a study in [31] that investigated the effect of surfactant concentration on the particle size of transferosomes containing paeonol. The authors of that study reported that increasing the surfactant concentration led to a decrease in particle size, which they attributed to the ability of the surfactant to solubilize within the lipid bilayer and reduce vesicle size, like the results of given studies.

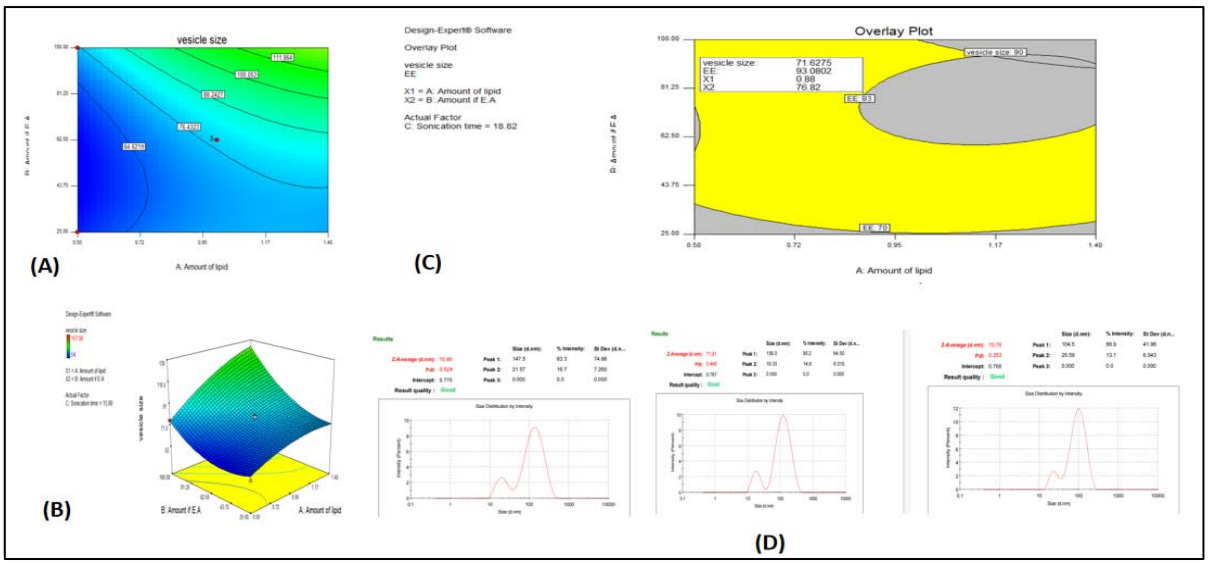

Fig. 5: A. Response surface plot for vesicle size of RTG B. Contour plot of vesicle size of RTG C. Overlay plot for checkpoint batch of RTG D. Vesicle size of checkpoint batch 1,2 and 3 of RTG

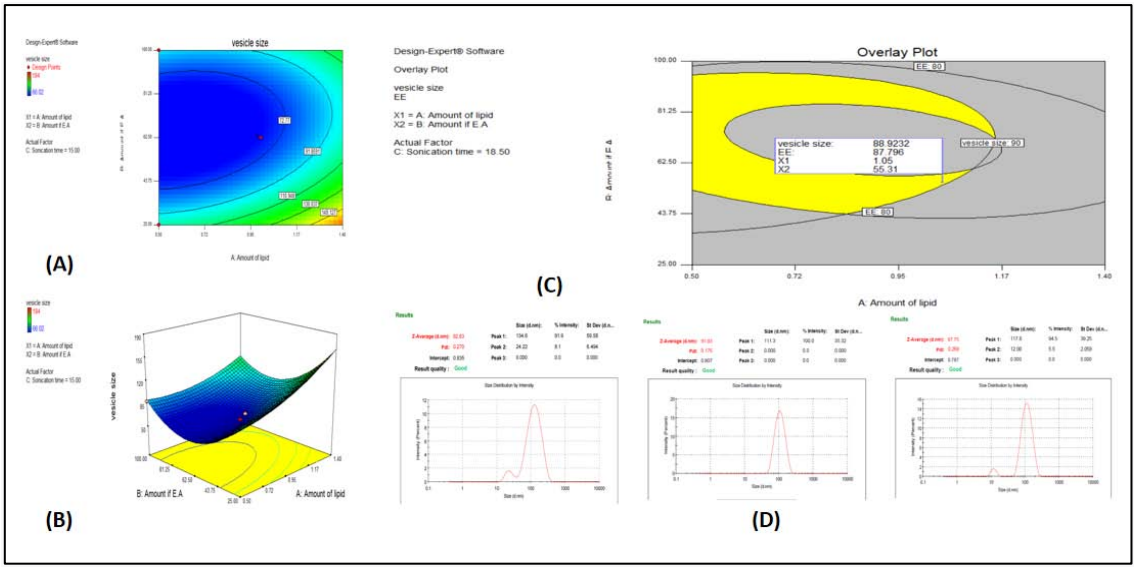

Fig. 6: A. Response surface plot for vesicle size of RSM B. Contour plot of vesicle size of RSM C. Overlay plot for check point batch of RSM D. Vesicle size of check point batch 1,2 and 3 of RSM

Entrapment efficiency

The results of this study regarding the positive correlation between lipid amount and drug entrapment efficiency are consistent with the findings of [32, 33], who also reported that higher lipid amounts lead to increased drug entrapment in transferosomes. However, the negative correlation between surfactant concentration and drug entrapment efficiency observed in this study contrasts with the results of [33], who reported that an increase in surfactant concentration led to higher drug entrapment. It is possible that differences in the types and amounts of lipids and surfactants used in these studies contributed to the observed differences in drug entrapment efficiency. The entrapment efficiency of RTG was found in the range of 45.66-88.96%, which indicates that some formulations have a high percentage of drug entrapment. The entrapment efficiency of RSM was found in the range of 57.6-92.57%, which suggests that some formulations have a high percentage of drug entrapment.

The polynomial equations were evaluated to analyse the variation in responses, such as vesicle size and entrapment efficiency for both RSM and RTG transferosomes. The variables A, B, and C represent the amounts of lipid, edge activator, and sonication period, respectively.

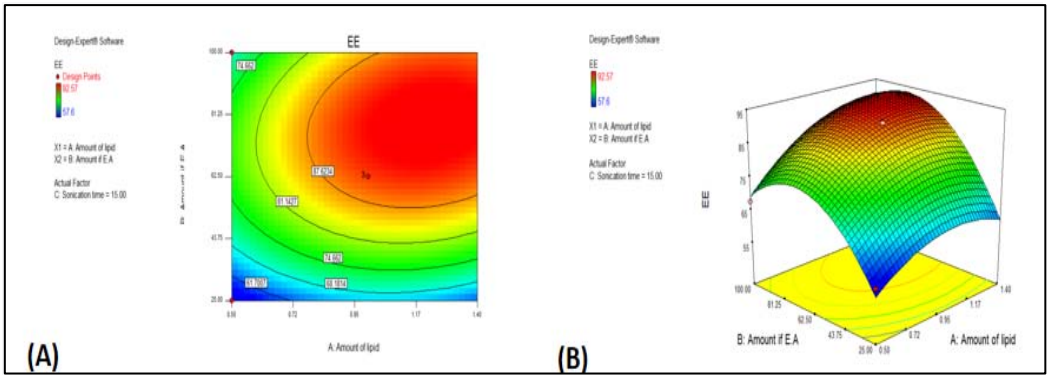

Fig. 7: A. Response surface plot for EE of RTG, B. Contour plot of EE of RTG

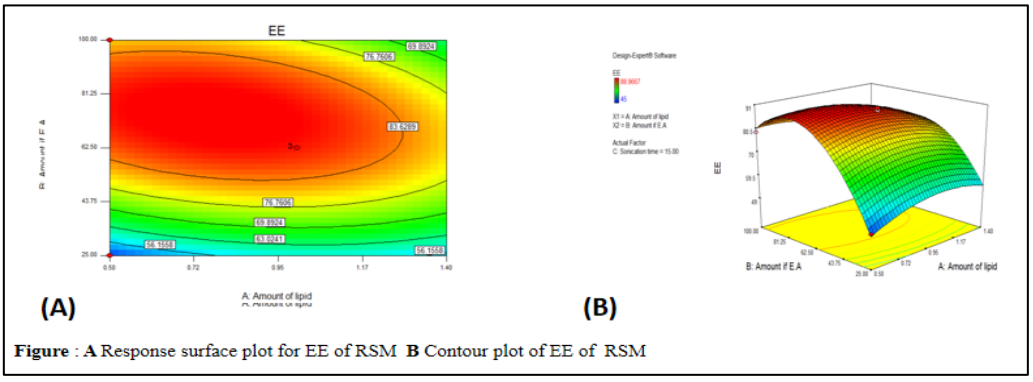

Fig. 8: A. Response surface plot for EE of RSM, B. Contour plot of EE of RSM

Polynomial equation variation in responses such as vesicle size and %EE was evaluated for RSM

Entrapment efficiency =+88.44–2.83*A+10.00* B+5.08*C-5.74*A*B+3.08*A*C-2.47 *B*C-5.71* A^2-20.53* B^2-3.46* C^2

Vesicle size =+64.24+23.26* A-15.24* B-12.19*C-9.37* A* B+4.38* A* C-2.52* B *C+13.16* A^2+42.95* B^2+44.63* C^2

Polynomial equation variation in responses such as vesicle size and %EE was evaluated for RTG

Vesicle size =+76.52+15.90* A+17.07* B-25.37*C+8.19* A * B-7.45* A* C–14.34* B* C-6.19* A^2+12.18* B^2+21.71* C^2

Entrapment efficiency =+89.81+6.74* A+10.28* B+5.16*C+3.30* A* B-1.72* A* C–1.41* B* C-6.64* A^2-14.23* B^2-1.50* C^2

These equations allow for the prediction of vesicle size and entrapment efficiency based on the amounts of lipid, edge activator, and sonication period used in the transferosome formulation. By varying the values of these variables, the optimal conditions for achieving the desired vesicle size and entrapment efficiency can be determined.

***In vitro* drug permeation studies**

Study in [34] reported the drug permeation of rotigotine hydrochloride using transpersonal dispersion and reported a cumulative drug release of 87.4% after 24 h using a Franz diffusion cell. Similarly, [35] investigated the drug permeation of rasagiline mesylate using transfersomal dispersion and reported a cumulative drug release of 89.1% after 24 h using a Franz diffusion cell. The current study investigated the drug permeation of optimized RTG and RSM transfersomal dispersion using a dialysis tube and found a higher cumulative permeation rate of 92.268% for RTG compared to previous work, but a slightly lower rate of 87.72% for RSM. These results indicate that transfersomal dispersion is an effective technique for promoting drug permeation, as demonstrated by the graphical representation of drug permeation results in fig. 9.

Table 2: Results of %EE and particle size for RTG and RSM transferosomes

Runs	Amount of lipid (g)	Amount of edge activator (mg)	Sonication time (min)	Rotigotine Hcl		Rasagiline mesylate	
				% E. E.	Vesicle size	% E. E.	Vesicle size
1	0.5	25	15	57.6±0.002	54.05±0.187	50.2±0.001	113.53±0.002
2	1.5	25	15	61.2±0.105	71.1±0.38	54.66±0.128	184.04±0.302
3	0.5	100	15	67.56±0.003	76.18±0.087	79.03±0.202	89.19±0.0112
4	1.5	100	15	85.84±0.106	129.7±0.312	58.12±0.005	118.73±0.003
5	0.5	62.5	10	65.16±0.001	96.7±0.015	81.5±0.213	106.18±0.011
6	1.5	62.5	10	81.45±0.004	141.8±0.227	64.23±0.003	162.99±0.002
7	0.5	62.5	20	83.93±0.004	59.3±0.31	84.19±0.002	83.34±0.421
8	1.5	62.5	20	92.57±0.562	71.81±0.387	80.93±0.012	159.46±0.004
9	1	25	10	58.23±0.001	107.76±0.087	45.66±0.005	178.8±0.001
10	1	25	20	65.97±0.122	84.9±0.187	61.76±0.001	150.28±0.403
11	1	100	10	86.34±0.001	167.98±0.007	71.3±0.143	163.9±0.005
12	1	100	20	88.45±0.005	87.75±0.027	78.2±0.004	125.3±0.01
13	1	62.5	15	90.4±0.401	78.8±0.107	87.96±0.001	68.2±0.005
14	1	62.5	15	90.64±0.001	78.07±0.312	87.23±0.003	66.02±0.112
15	1	62.5	15	90.4±0.205	77.76±0.001	88.96±0.125	66.75±0.212

Description: Data represents mean±SD (n=3)

Table 3: Results of %EE and particle size for RTG and RSM transfersomal check point batches

S. No.	Predicted results	Actual results for RTG transferosomes			Predicted Results	Actual results for RSM transferosomes		
		Batch 1	Batch 2	Batch 3		Batch 1	Batch 2	Batch 3
% EE	93.08	92.57±0.562	93.56±0.494	89.76±0.325	87.79	88.12±0.125	88.87±0.345	89.93±0.402
Vesicle size	71.62	70.88±0.107	71.81±0.387	70.76±0.721	88.92	92.63±0.613	91.03±0.241	91.75±0.501

Description: Data represents mean±SD (n=3)

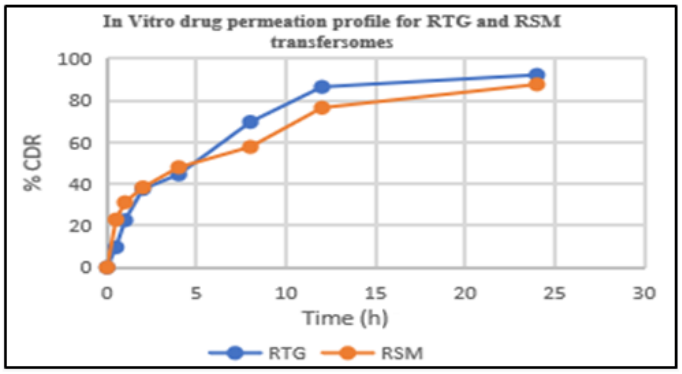

Fig. 9: Graphical representation of *in vitro* drug permeation profile for RTG and RSM transfersomes

% Deformability index

In a study conducted by [34] it was reported that the optimized transfersomal formulation of rotigotine hydrochloride, which was prepared using sodium cholate and span 80, had a deformability index of 94.6%. Another study found that the deformability index of the batch with vesicle size 211.06 nm was chosen and extruded from 0.20 m membrane and was found to be 115.78%. These results

suggest that the deformability index of transferosomes can be modified by adjusting the concentration and type of surfactants used in the formulation. Furthermore, these findings indicate that the deformability index plays an essential role in enhancing the permeation of drugs through the skin.

$$D = J\left(\frac{rv}{rp}\right)^2$$

$= 10.2(211.06/0.20)^2 = 115.78$ %

Where D = Deformability index, J = 10.2 ml extruded Transferosomal suspension, rv = 211.06 nm (0.211 µm) vesicular size of transferosomes after extrusion, rp = 0.20 µm pore size of membrane

Stability studies of transferosomes

Stability study of F8 to RTG and F14 of RSM was performed to assess the effect of storage at 4±2 °C for three months on the optimized transferosomal formulation. The observed vesicle size of F8 was 71.81±0.129 nm, % EE was 92.19±0.41 and for F14 66.01±0.129 nm, % EE was 87.19±0.71 (results are described in mean±SD, runs of analysis n=3).

CONCLUSION

A study was conducted to investigate the factors that affect the particle size and entrapment efficiency of transferosomes containing rotigotine HCL and rasagiline mesylate. Three significant factors, including lipid amount, edge activator amount, and sonication period, were identified and optimized using a Box-Behnken design. Various techniques were employed to characterize the optimized batch F8 for RTG and F15 for RSM, shows high entrapment efficiency, appropriate vesicle size, vesicle morphology and highest *In vitro* drug permeation after 24 h.

ACKNOWLEDGMENT

The authors are thankful to Neuland laboratory limited, Mumbai, India for proving Rotigotine HCl as gift sample.

FUNDING

Nil

AUTHORS CONTRIBUTIONS

Ms. Shivani Patel performed all the practical work and manuscript drafting. Dr. Lalit Lata Jha guided this project work and interpreted data for statistical analysis.

CONFLICT OF INTERESTS

The authors have no conflicts of interest regarding this investigation.

REFERENCES

1. Giladi N, Asgharnejad M, Bauer L, Grieger F, Boroojerdi B. Rotigotine in combination with the MAO-B inhibitor selegiline in early Parkinson's disease: A post hoc analysis. J Parkinsons Dis. 2016;6(2):401-11. doi: 10.3233/JPD-150758, PMID 27061066.
2. Elshoff JP, Cawello W, Andreas JO, Mathy FX, Braun M. An update on pharmacological, pharmacokinetic properties and drug–drug interactions of Rotigotine transdermal system in Parkinson's disease and restless legs syndrome. Drugs. 2015;75(5):487-501. doi: 10.1007/s40265-015-0377-y, PMID 25795100.
3. Jiang DQ, Wang HK, Wang Y, Li MX, Jiang LL, Wang Y. Rasagiline combined with levodopa therapy versus levodopa monotherapy for patients with Parkinson's disease: a systematic review. Neurol Sci. 2020;41(1):101-9. doi: 10.1007/s10072-019-04050-8. PMID 31446579.
4. Jalajakshi N, Chandrakala V, Srinivasan S. An overview: recent development in transdermal drug delivery. Int J Pharm Pharm Sci. 2022;14(10):1-9.
5. Chaurasiya P, Ganju E, Upmanyu N, Ray SK, Jain P. Transfersomes: a novel technique for transdermal drug delivery. J Drug Delivery Ther. 2019;9(1):279-85. doi: 10.22270/jddt.v9i1.2198.
6. Ezzat HM, Elnaggar YSR, Abdallah OY. Improved oral bioavailability of the anticancer drug catechin using chitosomes: design, *in vitro* appraisal and *in vivo* studies. Int J Pharm. 2019;565:488-98. doi: 10.1016/j.ijpharm.2019.05.034. PMID 31100382.
7. Chauhan P, Tyagi BK. Herbal novel drug delivery systems and transfersomes. J Drug Delivery Ther 2018;8(3):162-8. doi: 10.22270/jddt.v8i3.1772.
8. Moawad FA, Ali AA, Salem HF. Nanotransfersomes-loaded thermosensitive in situ gel as a rectal delivery system of tizanidine HCl: preparation, *in vitro* and *in vivo* performance. Drug Deliv. 2017;24(1):252-60. doi: 10.1080/10717544.2016.1245369, PMID 28156169.
9. Bnyan R, Khan I, Ehtezazi T, Saleem I, Gordon S, O'Neill FO. Surfactant effects on lipid-based vesicles properties. J Pharm Sci. 2018;107(5):1237-46. doi: 10.1016/j.xphs.2018.01.005, PMID 29336980.
10. Kumar A. Transferosome: a recent approach for transdermal drug delivery. J Drug Delivery Ther. 2023;8(5-s):100-4. doi: 10.22270/jddt.v8i5-s.1981.
11. Hjelmström P, Banke Nordbeck E, Tiberg F. Optimal dose of buprenorphine in opioid use disorder treatment: a review of pharmacodynamic and efficacy data. Drug Dev Ind Pharm. 2020;46(1):1-7. doi: 10.1080/03639045.2019.1706552. PMID 31914818.
12. Abraham P, Krupanidhi S, Rajeswara E, Indira M, Bobby M, Venkateswarulu TC. Plackett-Burman design for screening of process components and their effects on the production of lactase by newly isolated Bacillus sp. VUVD101 strain from Dairy effluent. Beni Suef Univ J Basic Appl Sci. 2018;7:543-6. doi: 10.1016/j.bjbas.2018.06.004.
13. Smith ZD, Keller JR, Bello M, Cordes NL, Welch CF, Torres JA. Plackett-Burman experimental design to facilitate syntactic foam development. J Appl Polym Sci. 2016;133(1). doi: 10.1002/app.42892.
14. Mueanmas C, Indum P. Application of Plackett-Burman design on screening the factors affecting torrefaction of palm kernel shell. IOP Conf Ser.: Earth Environ Sci. 2019;301(1):012030. doi: 10.1088/1755-1315/301/1/012030.
15. Ekpenyong MG, Antai SP, Asitok AD, Ekpo BO. Plackett-Burman design and response surface optimization of medium trace nutrients for glycolipopeptide biosurfactant production. Iran Biomed J. 2017;21(4):249-60. doi: 10.18869/acadpub.ibj.21.4.249, PMID 28433004.
16. Sahu PK, Ramisetti NR, Cecchi T, Swain S, Patro CS, Panda J. An overview of experimental designs in HPLC method development and validation. J Pharm Biomed Anal. 2018;147:590-611. doi: 10.1016/j.jpba.2017.05.006. PMID 28579052.
17. Deka T, Das MK, Das S, Das P, Singha LR. Box-Behnken design approach to develop nano-vesicular herbal gel for the management of skin cancer in experimental animal model. Int J App Pharm. 2022;14(6):148-66. doi: 10.22159/ijap.2022v14i6.45867.
18. Tamilarasan N, Yasmin BM, Anitha P, Umme H, Cheng WH, Mohan S. Box-Behnken design: optimization of proanthocyanidin-loaded transferosomes as an effective therapeutic approach for osteoarthritis. Nanomaterials (Basel). 2022;12(17):2954. doi: 10.3390/nano12172954, PMID 36079990.
19. Jangdey MS, Gupta A, Saraf S, Saraf S. Development and optimization of apigenin-loaded transfersomal system for skin cancer delivery: *in vitro* evaluation. Artif Cells Nanomed Biotechnol. 2017;45(7):1452-62. doi: 10.1080/21691401.2016.1247850, PMID 28050929.
20. Magdy I, Amna M, Makky A, Menna M. Formulation and characterization of ethosomes bearing vancomycin hydrochloride for transdermal delivery. Int J Pharm Pharm Sci. 2014;6(11):190-4.
21. Varia U, Joshi D, Jadeja M, Katariya H, Detholia K, Soni V. Development and evaluation of ultradeformable vesicles loaded transdermal film of boswellic acid. Futur J Pharm Sci. 2022;8(1):39. doi: 10.1186/s43094-022-00428-2.
22. Anitha P, Ramkanth S, Satyanarayana SV. QBD based design and characterization of proniosomal transdermal delivery of atenolol and glibenclamide combination: an innovative approach. Bull Fac Pharm Cairo Univ. 2021 Jan;59(1):11-26. doi: 10.54634/2090-9101.1021.

23. Ramkanth S, Anitha P, Gayathri R, Mohan S, Babu D. Formulation and design optimization of nano-transferosomes using pioglitazone and eprosartan mesylate for concomitant therapy against diabetes and hypertension. Eur J Pharm Sci. 2021;162:105811. doi: 10.1016/j.ejps.2021.105811, PMID 33757828.
24. Banu R, Gerding J, Franklin C, Sikazwe D, Horton W, Torok M. 4,5-Dimethoxy-2-nitrobenzohydrazides and 1-(1-Benzylpiperidin-4-yl)ethan-1-ones as potential antioxidant/cholinergic endowed small molecule leads. Sci Pharm. 2017;86(1):2. doi: 10.3390/scipharm86010002, PMID 29267246.
25. Ko JH, Sethi G, Um JY, Shanmugam MK, Arfuso F, Kumar AP. The role of resveratrol in cancer therapy. Int J Mol Sci. 2017;18(12):2589. doi: 10.3390/ijms18122589, PMID 29194365.
26. Mondal A, Bennett LL. Resveratrol enhances the efficacy of sorafenib mediated apoptosis in human breast cancer MCF7 cells through ROS, cell cycle inhibition, caspase 3 and PARP cleavage. Biomed Pharmacother. 2016;84:1906-14. doi: 10.1016/j.biopha.2016.10.096, PMID 27863838.
27. Zubiaur P, Matas M, Martin Vilchez S, Soria Chacartegui P, Villapalos Garcia G, Figueiredo Tor L. Polymorphism of drug transporters, rather than metabolizing enzymes, conditions the pharmacokinetics of rasagiline. Pharmaceutics. 2022;14(10):2001. doi: 10.3390/pharmaceutics14102001, PMID 36297437.
28. Ibrahim SS, Abo Elseoud OG, Mohamedy MH, Amer MM, Mohamed YY, Elmansy SA. Nose-to-brain delivery of chrysin transfersomal and composite vesicles in doxorubicin-induced cognitive impairment in rats: insights on formulation, oxidative stress and TLR4/NF-kB/NLRP3 pathways. Neuropharmacology. 2021;197:108738. doi: 10.1016/j.neuropharm.2021.108738, PMID 34339751.
29. Song X, Chen Z, Liu Y. MicroRNA-134 contributes to glucose-induced endothelial injury via targeting ARNT in human umbilical vein endothelial cells. Yonsei Med J. 2018;59(3):455-63. doi: 10.3349/ymj.2018.59.3.455.
30. Elsayed MM, Abdallah OY, Naggar VF, Khalafallah NM. Lipid vesicles for skin delivery of drugs: reviewing three decades of research. Int J Pharm. 2007;332(1-2):1-16. doi: 10.1016/j.ijpharm.2006.12.005. PMID 17222523.
31. Zhou X, Zhang Z, Li Y, Hao Y, Li S, Wu C. Advances in liposomal drug delivery system decorated with cell-penetrating peptides for cancer treatment. Curr Pharm Des. 2017;23(3):302-11.
32. Sharma P, Garg S, Purewal TS. Solid lipid nanoparticles (SLNs) and nanostructured lipid carriers (NLCs) for pulmonary drug delivery: a review. J Microencapsul. 2018;35(2):131-42.
33. Sarwa KK, Suresh PK, Yadav P. Development and evaluation of mucoadhesive microemulsion of terbinafine hydrochloride for the treatment of onychomycosis. J Microencapsul. 2017;34(1):22-33.
34. El-Sabawi D, Abu-Dahab R, Zalloum WA, Ijbara F, Hamdan II. The effect of ferrous ions, calcium ions and citric acid on absorption of ciprofloxacin across caco-2 cells: practical and structural approach. Drug Dev Ind Pharm. 2019;45(2):292-303. doi: 10.1080/03639045.2018.1539495. PMID 30348012.
35. Patel N, Desai R, Patel D. Preparation and evaluation of transfersomes containing rasagiline mesylate for transdermal delivery. J Drug Deliv Sci Technol. 2021;61:102116.